

Expanded View Figures

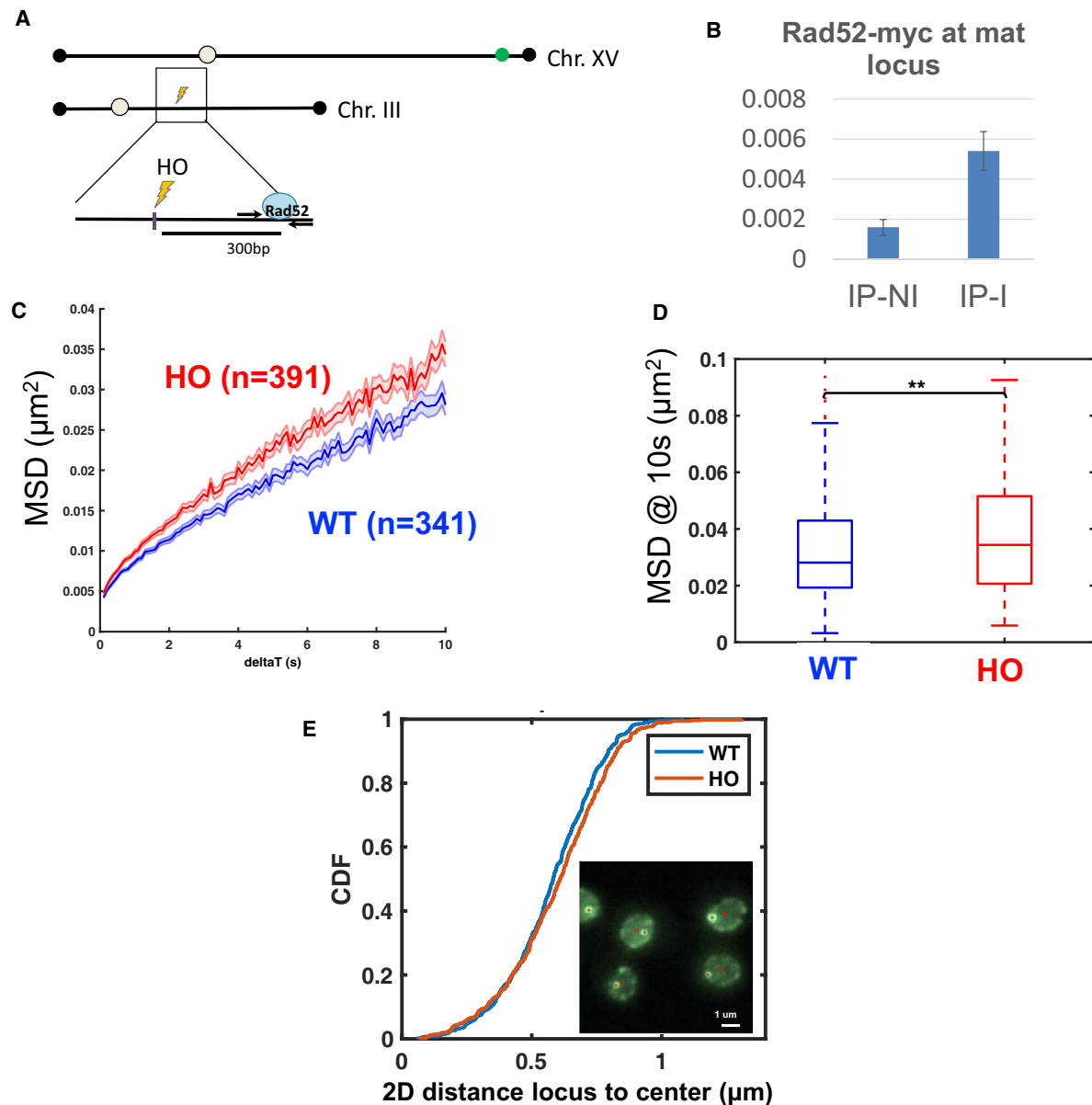


Figure EV1. Localized double-strand break increases chromatin mobility on other chromosomes.

- A** Schematic showing the position of the HO (homothallic switching endonuclease) cutting site at the MAT locus on chromosome III (lightning symbol) and the Tet operator sequence in the subtelomeric region of chromosome XV, which is targeted by TetR-GFP (green dot). Rad52 monitors repair by homologous recombination upon HO induction.
- B** Chromatin immunoprecipitation for Myc-tagged Rad52 at the MAT locus monitored by Q-PCR after 1 h of HO induction (IP-I) as compared to non-induction (IP-NI). Expression of endonuclease HO is driven by a galactose (GAL1-10) promoter. Bars show averages of 3 replicate experiments, and error bars show standard deviations.
- C** Mean square displacements of the TetR-GFP labeled locus (population median). Blue: cells not expressing HO and grown in galactose ($n = 341$ cells). Red: cells expressing HO, after 1 h induction in galactose ($n = 391$ cells). The shaded area is the interquartile range divided by $\sqrt{(n)}$.
- D** Boxplots show the distribution of MSD at 10 s in the presence or absence of HO induction. A Wilcoxon rank-sum test between distributions indicates significant increase upon induction ($**P < 0.01$). The horizontal line at the center of each box indicates the median value, the bottom and top limits indicate the lower and upper quartiles, respectively. The whiskers indicate the full range of measured values.
- E** Distribution of distances between the locus and the nuclear center, for cells expressing HO endonuclease ($n = 509$, red) and cells not expressing HO ($n = 569$, blue). A rank-sum test detected no significant differences ($P = 0.08$). Inset shows a few cells, with the bright GFP spot marked by a red cross and the nuclear center by a red circle. Distances were measured on 2D projections of 3D z-stacks.

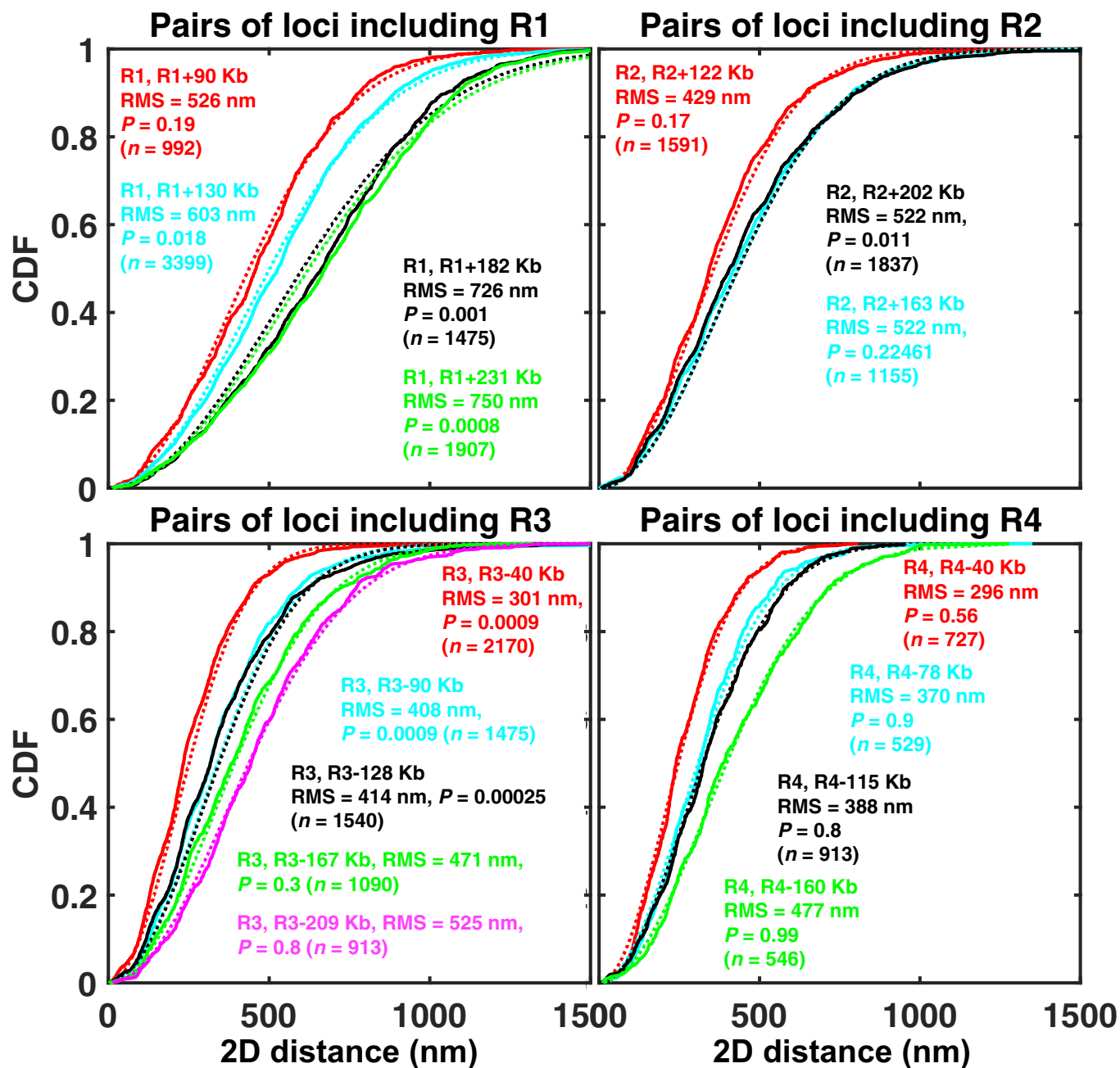


Figure EV2. Distribution of distances between 16 pairs of chromatin loci in the absence of Zeocin.

Each panel corresponds to a different reference locus (R1, R2, R3, or R4), as indicated. Each solid curve is the empirical cumulative distribution function (CDF) for the pair of loci indicated in the same-colored legend. The dotted curve of the same color shows the function $F(R; R_0) = 1 - \exp(-R^2/R_0^2)$, where $R_0 = \langle R^2 \rangle^{1/2}$, is the experimentally measured root-mean square (RMS) distance, measured between the two loci, as indicated in the legend. F is the CDF expected for a Gaussian distribution of the distance vector between the two loci, as predicted by an ideal chain model (see Appendix Supplementary Methods). The P -value indicates the result of a Kolmogorov–Smirnov test comparing the experimentally measured CDF to F . For nine out of 16 pairs, the measured CDF is statistically undistinguishable from the Gaussian model ($P > 0.05$), for two more, the difference is only marginally significant ($P > 0.01$). The number of cells for each pair, n , is indicated.

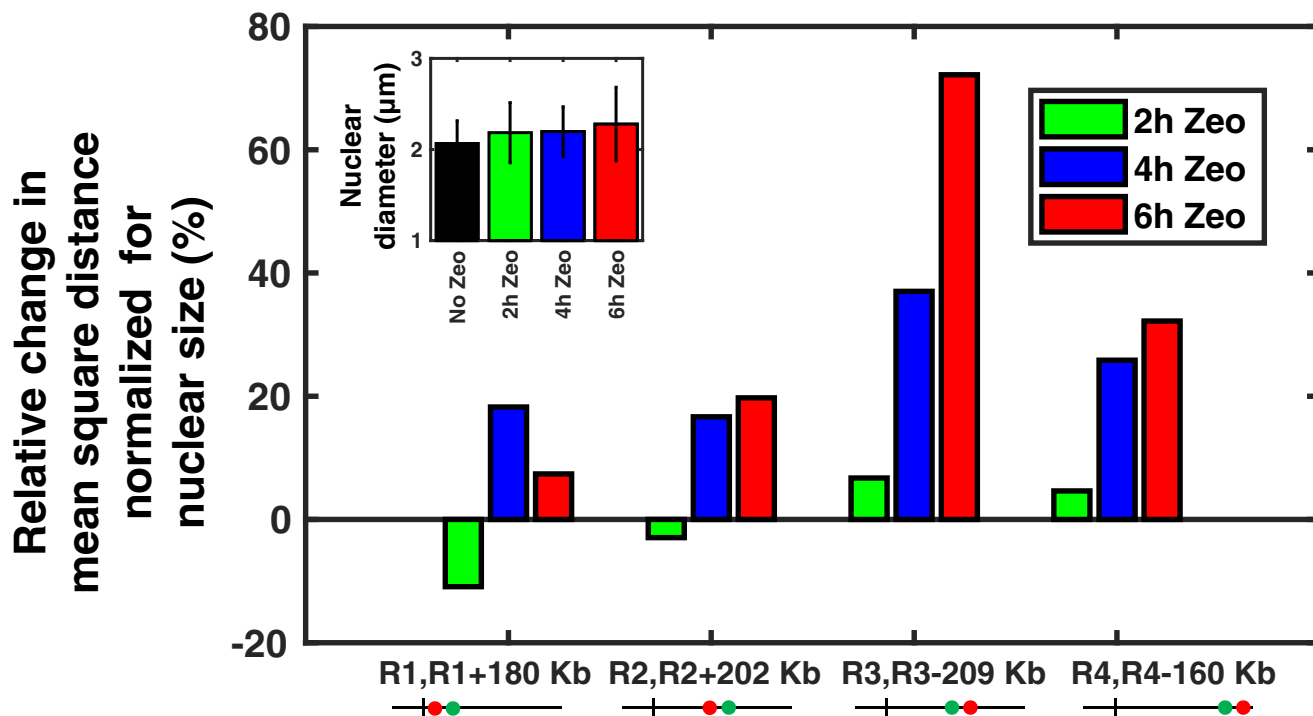


Figure EV3. Prolonged Zeocin treatment increases intrachromosomal distances.

Relative change in mean square distances between pairs of loci (in %), as in Fig 3B, but after normalization by the mean nuclear diameter for each Zeocin exposure, as shown in the inset (diameter was measured in cells with fluorescently tagged nuclear envelope; error bars show standard deviations).

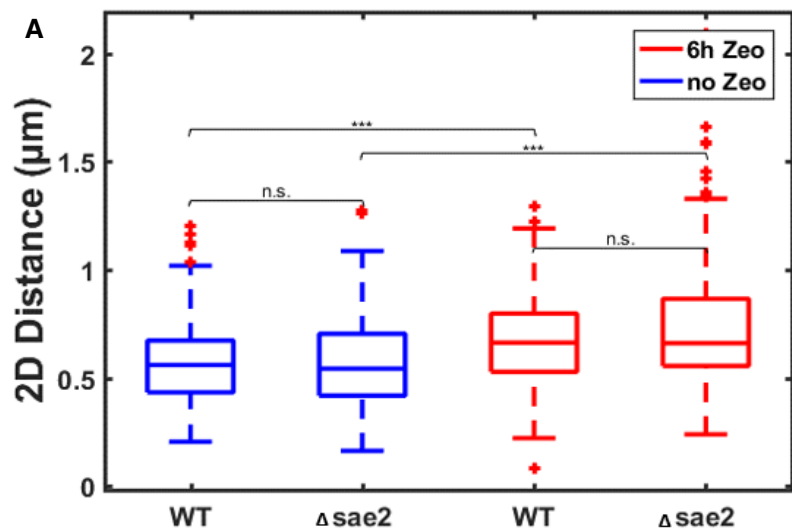
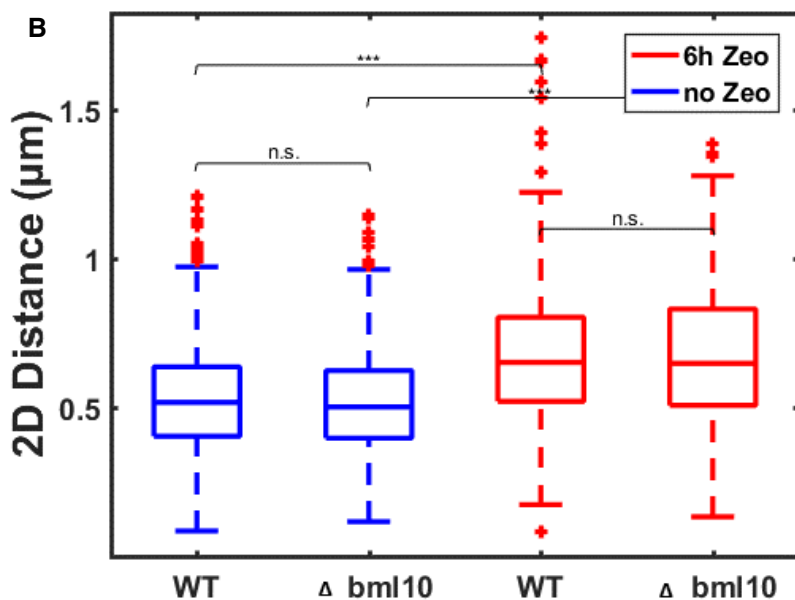


Figure EV4. Proteins Sae2 and Blm10 do not contribute to the Zeocin-dependent increase in intrachromosomal distances.

A Boxplots show the distributions of 2D intrachromosomal distances between loci R3 and R3-167 kb (see Fig 1B) in a deletion mutant of Sae2 (Δ sae2) as compared to wild-type cells (WT), in untreated cells (blue) or in cells exposed to Zeocin for 6 h (red).

B Same as (A) but for the deletion mutant of Blm10 (Δ blm10).

Data information: The horizontal line at the center of each box indicates the median value, the bottom and top limits indicate the lower and upper quartiles, respectively. The whiskers indicate the full range of measured values, except for outliers, which are shown as red crosses. Brackets indicate the results of a Wilcoxon rank-sum test on pairs of distributions, with "n.s." for not significant ($P > 0.05$), and *** for $P < 0.001$.



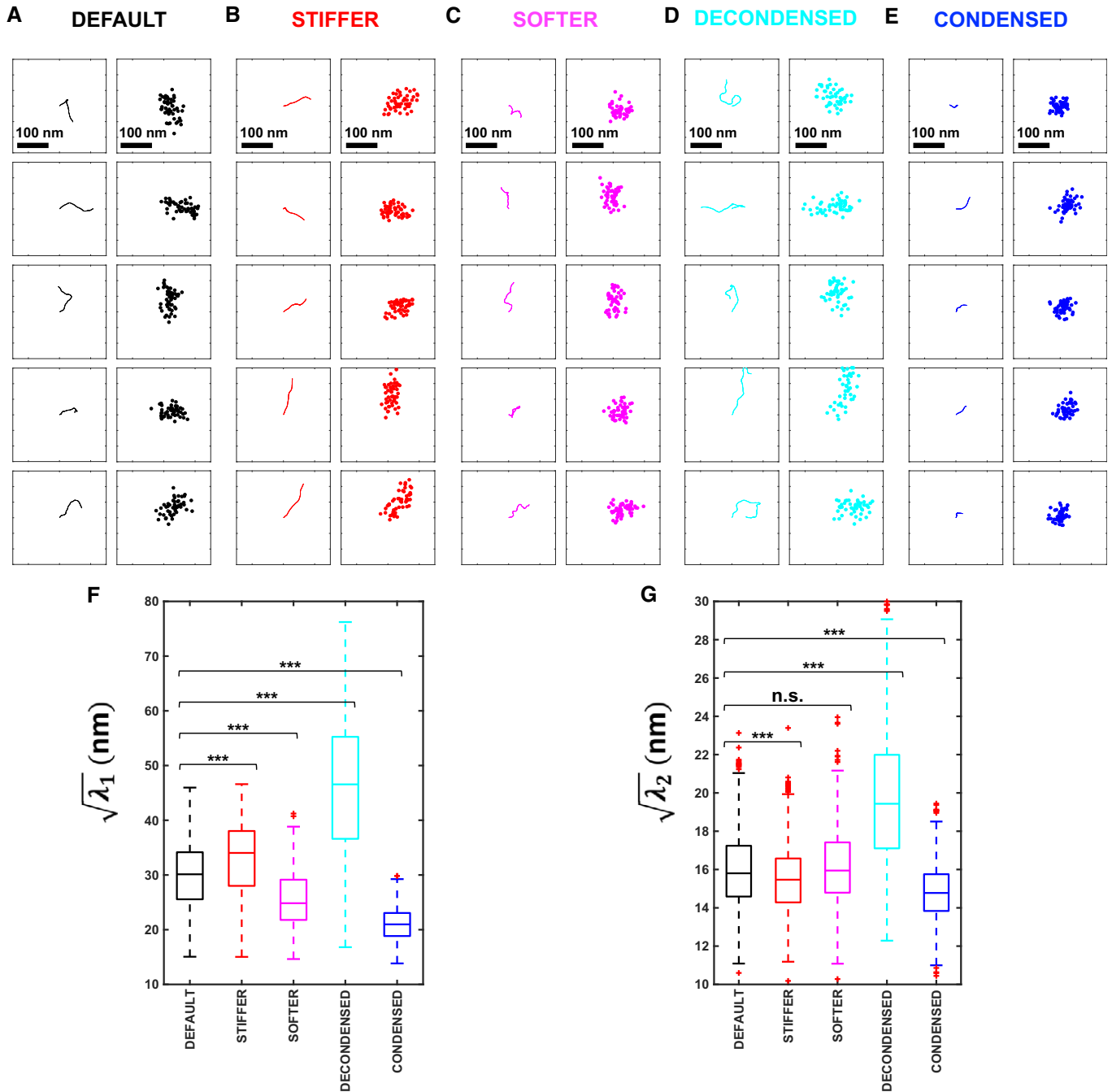


Figure EV5. Shape analysis of a super-resolved chromatin fiber region can distinguish between decondensation and stiffening.

- A** Five simulated configurations of a 7-kb chromatin region (left column) and corresponding single-molecule localizations (right column). The simulated configurations are 2D projections of 3D freely rotating chains with a persistence length of $P_0 \approx 70$ nm and a compaction of $C_0 \approx 50$ bp/nm, implying a contour length ≈ 140 nm (below the diffraction limit to optical resolution). Localization clouds $(x_i, y_i)_{i=1..n}$ were simulated by randomly sampling $n = 50$ positions along the chain and adding normally distributed random positioning errors with standard deviation $\sigma \approx 15$ nm.
- B** Same as panel (A), but for a stiffer fiber, with $P \approx 180$ nm and $C = C_0$.
- C** Same as panel (A), but for a softer fiber, with $P \approx 27$ nm and $C = C_0$.
- D** Same as in panel (A), but for a less compact (decondensed) fiber, with $P = P_0$ and $C = C_0/2 \approx 25$ bp/nm.
- E** Same as in panel (A), but for a more compact (condensed) fiber, with $P = P_0$ and $C = 2C_0 \approx 100$ bp/nm.
- F, G** Boxplots show the distributions of $\sqrt{\lambda_1}$ and $\sqrt{\lambda_2}$ for 1,000 configurations in each of the five scenarios. The horizontal line at the center of each box indicates the median value, the bottom and top limits indicate the lower and upper quartiles, respectively. The whiskers indicate the full range of measured values, except for outliers, which are shown as red crosses. Brackets indicate the results of a Wilcoxon rank-sum test on pairs of distributions, with "n.s." for $P > 0.05$ (not significant), and *** for $P < 0.001$.